

pubs.acs.org/Macromolecules Article

Topological Simplification of Complex Knots Untied in Elongational Flows

Beatrice W. Soh, Alexander R. Klotz, and Patrick S. Doyle*



Cite This: Macromolecules 2020, 53, 7389-7398



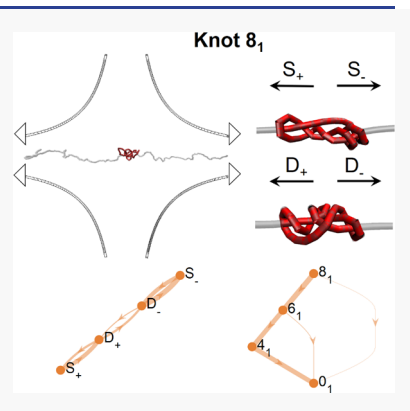
ACCESS

Metrics & More

Article Recommendations

Supporting Information

ABSTRACT: We use Brownian dynamics simulations to study the topological simplification of knots that untie from chains in elongational flows. Focusing on the 81 knot, we track changes in conformational states as initially centered knots move off chains in planar elongational flows. We show that the non-uniform tension profile along the chain leads to a redistribution of conformational states at different knot locations along the chain. The rotational mode of motion for knots in elongational flows promotes a preferred knot conformational state rearrangement pathway, which results in a dominant untying pathway. The interplay between chain tension, conformational state rearrangement pathway and knot untying time is further probed by varying chain length. Finally, we generalize our findings by considering the untying pathways of other twist knots in elongational flows. From a practical standpoint, using flow kinematics to influence the topological simplification pathway of a knot can be potentially exciting for single-molecule applications.



1. INTRODUCTION

Polymer chain entanglements on the microscopic scale can significantly impact the macroscopic behavior of the polymer system. The topic of chain entanglement has been of interest to polymer scientists for decades. A minimal system for studying chain entanglement is a self-entanglement, or a knot. Knots are ubiquitous in our daily lives over a wide range of length scales spanning from sailing knots to proteins, habitation is unsurprising given the inevitability of knots in long chains. The impact of knots on polymer dynamics has been investigated in a wide range of experimental and computational studies. The impact of service of experimental and computational studies.

From a mathematical perspective, the topological state of a knot is well-defined only in a closed curve. However, linear chains with free ends can also contain localized, distinct knots. The interest in polymer knots has led to investigation into the process of knotting and, recently, unknotting of linear chains. Long polymer chains in equilibrium can spontaneously form knots when either a chain end or a hairpin bend followed by a chain end threads through a loop on the same chain, with the knotting mechanism influencing where the knot appears along the chain. 13,14 Conversely, a polymer can become unknotted when thermal fluctuations cause the knot to diffuse off a chain end. 15 Studies by our group have shown that subjecting a knotted polymer to an elongational flow results in convective transport of the knot off the chain and can facilitate the unknotting process. ^{16–18} From a nanotechnology application standpoint, the untying of knots on polymer chains is of interest to next-generation DNA mapping and sequencing technologies, for which the presence of knots can lead to erroneous nucleotide reads. ^{7,19,20}

The focal points of most polymer unknotting studies to date have been the mechanism of knots moving off chains and unknotting dynamics. ^{13,14,16,17,21} The topological simplification that a complex knot undergoes as it unties has been largely overlooked, yet is an important aspect of the unknotting process that can provide insight into how knots form and untie on polymer chains. The important role that knots play in the stability and folding pathway of proteins ^{22,23} has garnered interest in probing how knots on proteins untie, which can guide the understanding of how knotted proteins fold. ^{24,25} The topological pathway of knots has also been considered in studies seeking to understand local reconnection events that drive the topological simplification of knots, ranging from the enzymatic action of type II topoisomerase in unknotting DNA ^{26,27} to vortex reconnections that disentangle knotted vortices in fluids. ^{28,29}

A recent computational study by our group 30 examined the topological pathways of knots untying from uniformly tensioned chains. Focusing on the 8_1 knot as a model knot, we observed the rearrangement of conformational states as the knot moved off the chain and rationalized the observed distribution of knot untying pathways based on the distribution of knot conformational states. Given that flow kinematics influence the unknotting process, it is compelling to investigate

Received: June 8, 2020 Revised: August 5, 2020 Published: August 20, 2020





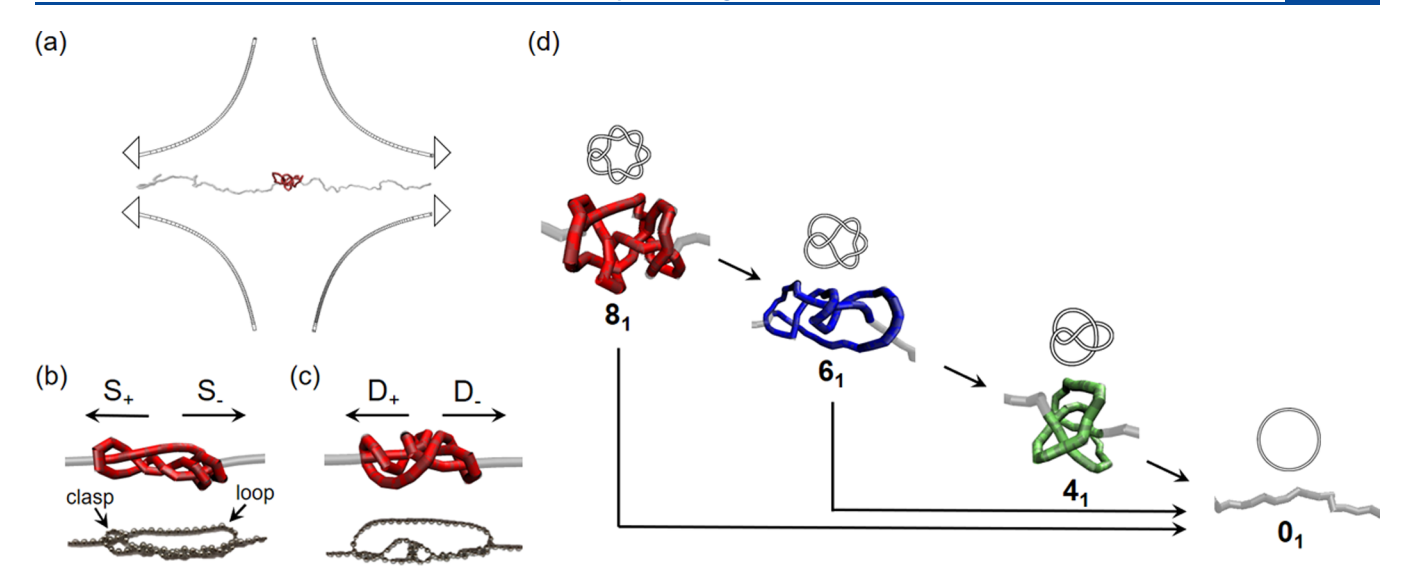


Figure 1. (a) Schematic of simulation setup: polymer chain with a 8_1 knot (red) in a planar elongational flow. (b, c) Conformational states for the 8_1 knot in an elongational flow: S_+ , S_- , D_+ , and D_- . Top: simulation snapshots. Bottom: images of macroscale chains. "Loop" and "clasp" of the knot as labeled. (d) Possible untying pathways for the 8_1 knot.

the topological mechanism of untying knots in non-equilibrium flows. In this work, we use Brownian dynamics simulations to study the untying pathways of knots in planar elongational flow, one of the simplest and most commonly studied flow types. As in our previous study,³⁰ we choose to focus first on the 81 knot and then generalize our findings to other knots. The 81 knot is selected because of its sufficient complexity for rich untying dynamics and well-studied conformational states. We subject chains with the 81 knot to planar elongational flows of varying strengths and track the conformational states as the knots move off the chains. The non-uniform chain tension profile results in different distributions of conformational states as the knot translates along the chain. The rotation of knots in elongational flows promotes a preferred conformational state rearrangement pathway and, consequently, a dominant untying pathway for the knot.

2. METHODS

2.1. Numerical Simulation. We performed Brownian dynamics simulations for linear, touching-bead chains to model polymers in planar elongational flows. Each polymer chain consisted of N=300 beads with diameter b at positions \mathbf{r}_b connected by N-1 rigid rods of length l=b=10 nm. The governing stochastic differential equation was derived by considering the relevant forces acting on the system: excluded volume, hydrodynamic, constraint, and Brownian.

The excluded volume potential, which gives rise to short-range repulsions between beads, was implemented to prevent self-crossings and can be described as

$$E^{\text{ev}} = -\sum_{i,j}^{N} \mu r_{ij} \text{ if } r_{ij} < b$$

where μ = 35 pN has been demonstrated to result in a low frequency of chain crossings.^{31,32} The force is then obtained as

$$\mathbf{F}_{i}^{\mathrm{ev}} = -\sum_{i}^{N} \mu \text{ if } r_{ij} < b$$

We neglected hydrodynamic interactions between the beads, so the drag force on the *i*th bead is given by

$$\mathbf{F}_{i}^{d} = \zeta \left(\mathbf{u}(\mathbf{r}_{i}) - \frac{\mathrm{d} \mathbf{r}_{i}}{\mathrm{d} t} \right)$$

where ζ is the drag coefficient of a single bead and $u(r_i)$ is the unperturbed solvent velocity. The constraint force takes the form

$$\mathbf{F}_{i}^{c} = T_{i}\mathbf{b}_{i} - T_{i-1}\mathbf{b}_{i-1}$$

where \mathbf{b}_i is the unit vector of bond i and T_n is the tension in rod i that enforces the constraint of constant bond length. The Brownian forces are random forces that satisfy the fluctuation—dissipation theorem, described by

$$\langle \mathbf{F}_{i}^{\mathrm{br}}(t) \rangle = 0 \text{ and } \langle \mathbf{F}_{i}^{\mathrm{br}}(t) \mathbf{F}_{j}^{\mathrm{br}}(t) \rangle = \frac{2k_{\mathrm{b}}T\zeta\mathbf{I}\delta_{ij}}{\Delta t}$$

where δ_{ij} is the Kronecker delta, I is the identity matrix, and Δt is the simulation time step.

With the neglect of chain inertia, the sum of forces on the beads was set to zero. This led to the Langevin equation that describes the motion of each bead on the chain:

$$\frac{\mathrm{d} \mathbf{r_i}}{\mathrm{d} t} = \mathbf{u}(\mathbf{r_i}) + \frac{1}{\zeta} (\mathbf{F}_i^{\mathrm{ev}} + \mathbf{F}_i^{\mathrm{c}} + \mathbf{F}_i^{\mathrm{br}})$$

We employed a predictor—corrector scheme, discussed in detail by Liu et al.³³ to determine the bead positions at each time step. Imposing the rigid rod constraints results in a system of nonlinear equations for the rod tensions T_{ij} which were solved for using Newton's method.³⁴

In the simulations, we tied a knot into the center of the polymer chain and extended the knotted chain in a planar elongational flow of the form $\mathbf{u}(\mathbf{r}_i) = \dot{\varepsilon}(\hat{\mathbf{x}}\hat{\mathbf{x}} - \hat{\mathbf{y}}\hat{\mathbf{y}}) \cdot \mathbf{r}_i$, where $\dot{\varepsilon}$ is the strain rate and $\hat{\mathbf{x}}$ and $\hat{\mathbf{y}}$ are unit vectors parallel to the x and y axes, respectively (Figure 1a). The response of molecules in an elongational flow is typically characterized by the Weissenberg number, which represents the ratio of elastic to viscous forces. The Weissenberg number is defined as Wi = $\dot{\varepsilon}\tau$, where τ is the longest relaxation time of the unknotted molecule and can be obtained from a single-exponential fit to the last 30% extension of an initially stretched chain. We note that the presence of a knot reduces the relaxation time of a molecule and consequently results in a decrease in effective Wi.4 For a given set of simulation parameters, the knotted chain was equilibrated at the simulation conditions for between $10^4 \tau_d$ and $4 \times 10^5 \tau_d$ with τ_d = $l^2\zeta/k_hT$ being the characteristic rod diffusion time. During chain equilibration, the position of the knot was held at the center of the chain via reptation moves, in which a segment was cut off from one

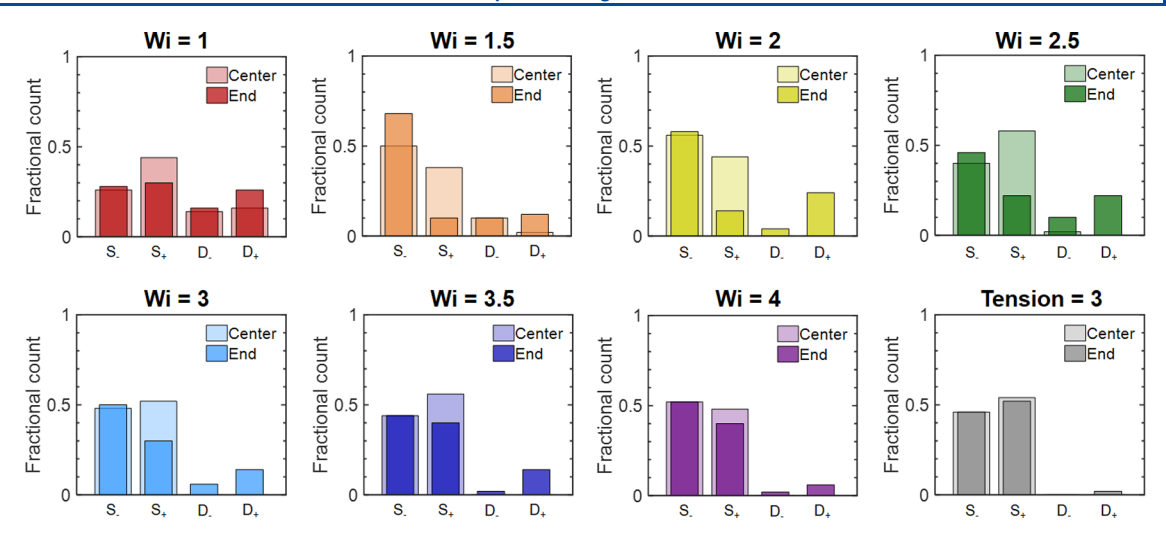


Figure 2. Distributions of conformational states of the 8_1 knot at the center versus end of the chain in elongational flows at different Wi. The isotension case is shown for comparison purposes. An ensemble of 50 chains was run for each Wi.

end of the chain and appended to the other end. 17,30 After equilibration, we ran the simulations until the initially centered knot moved off the chain using a time step of $\Delta t = 5 \times 10^{-4} \tau_d$. See the Supporting Information for representative simulation movies.

2.2. Knot Detection and Untying Pathway. The algorithm for detecting the topology of a knotted chain is detailed in previous studies by our group^{16,17,30} and briefly summarized. The chain ends of the knotted polymer were first connected together with an auxiliary arc, constructed using the minimally interfering closure scheme to minimize the introduction of additional entanglement during chain closure.³⁵ The chain conformation was projected onto a plane parallel to the elongational axis, following which chain crossings were identified and the Alexander polynomial was evaluated to determine the chain topology.³⁶ The boundaries of the knot were identified by determining the smallest subset of the chain that had the same topology as the whole chain.

In this study, we focus on the elongational flow-induced untying of the 81 knot as a model knot. The 81 knot belongs to the family of twist knots, which are generated by forming a link between the ends of a closed loop that has been twisted a number of times.³⁷ There are two possible conformational states for the 81 knot ["S" (single clasp) and "D" (double clasp)] that can be smoothly deformed into the other via rearrangements of certain strands without the knot type being changed.³⁰ On a uniformly tensioned chain, knot motion is governed by diffusion and thus lacks directionality. For an extended chain in an elongational flow, beyond a finite distance from the center of the chain, knot motion is driven by convection and has a fixed directionality of translation.¹⁶ Therefore, we take into account the direction of knot motion and further differentiate the conformational states of the 8₁ knot into "S₊", "S₋", "D₊", and "D₋" (Figure 1b,c). The S₊ and S₋ states are energetically equivalent, as are the D₊ and D₋ states, with the only difference being the orientation of the knot with respect to the direction of knot motion. For a given run, the direction of knot motion is fixed and taken to be the overall direction in which the knot moves to eventually reach a chain end. We emphasize that the knot only takes on one overall direction of motion per run, such that the changes in direction that result from diffusive motion of the knot would not affect the conformational state. As knot motion on a uniformly tensioned chain is not directed, the differentiation between the S₊ and S₋ or D₊ and D₋ states is not meaningful, but we maintain the classification scheme for consistency.

The way in which the 8_1 knot unties depends on the knot conformational state it is in when a chain end is reached. In the S_+ state, the knot comes off the chain end at the clasp and unties completely in a single step; in the S_- state, it unties in three steps, assuming no further rearrangement of the partially untied knot. In the D_+ state, the knot comes off the chain end with fewer twists and

unties in two steps; in the D_- state, it unties in three steps. In terms of the knot untying pathway (Figure 1d), an 8_1 knot in the S_+ state will completely untie to the 0_1 knot and in the S_- state will partially untie to the 6_1 knot, followed by the 4_1 knot and the 0_1 knot. An 8_1 knot in both D_+ and D_- states will partially untie to the 6_1 knot, followed by either the 0_1 knot for the D_+ state or the 4_1 knot and then the 0_1 knot for the D_- state. See Figures S1 and S2 for visual illustrations.

To determine the conformational state of the 81 knot, we performed crossing switches at both ends of the knot boundaries. A crossing switch involves changing a strand from being over to under another strand at a crossing, or vice versa, and is equivalent to a knot passing through itself to untie once. By evaluating the chain topology after performing a crossing switch on each end of the knot boundary, we were able to determine whether the knot was in a S or D state. Specifically, a crossing switch at the boundary of a 8_1 knot in the S states would give an unknot at one end and the 61 knot at the other end, whereas a crossing switch at the boundary of a 81 knot in the D states would result in the 61 knot at either end. This protocol is sufficient for distinguishing between the S+ and S- states due to the different chain topologies that result from crossing switches at either end of the knot boundary. To discriminate between the D+ and Dstates, we further performed crossing switches at the next closest crossing to each end of the knot boundary. For an 81 knot in the D states, this would yield an unknot at one end and the 41 knot at the other end. Since the identified knot boundaries and, hence, the detected knot conformational state can depend on how the chain crossings were projected onto the plane, we performed the conformational state detection procedure with the knot projected onto 200 different planes at each time step, from which we recorded the most frequently detected conformational state. The accuracy of the algorithm was verified by visual inspection.

3. RESULTS AND DISCUSSION

3.1. Conformational State Rearrangement Pathway.

A knot on a chain subjected to a constant tension force diffuses along the chain until it reaches a chain end and unties. We recently demonstrated³⁰ that thermal fluctuations can induce conformational state rearrangements of a knot and that the probability of a knot being in a given conformational state depends on the applied chain tension. For the model 8₁ knot, the knot predominantly assumes the S state for non-zero chain tensions, with the probability of being in the S state increasing with increasing tension.

In an elongational flow, the knot untying process can be diffusion-driven or convection-driven. ¹⁷ Given that the tension

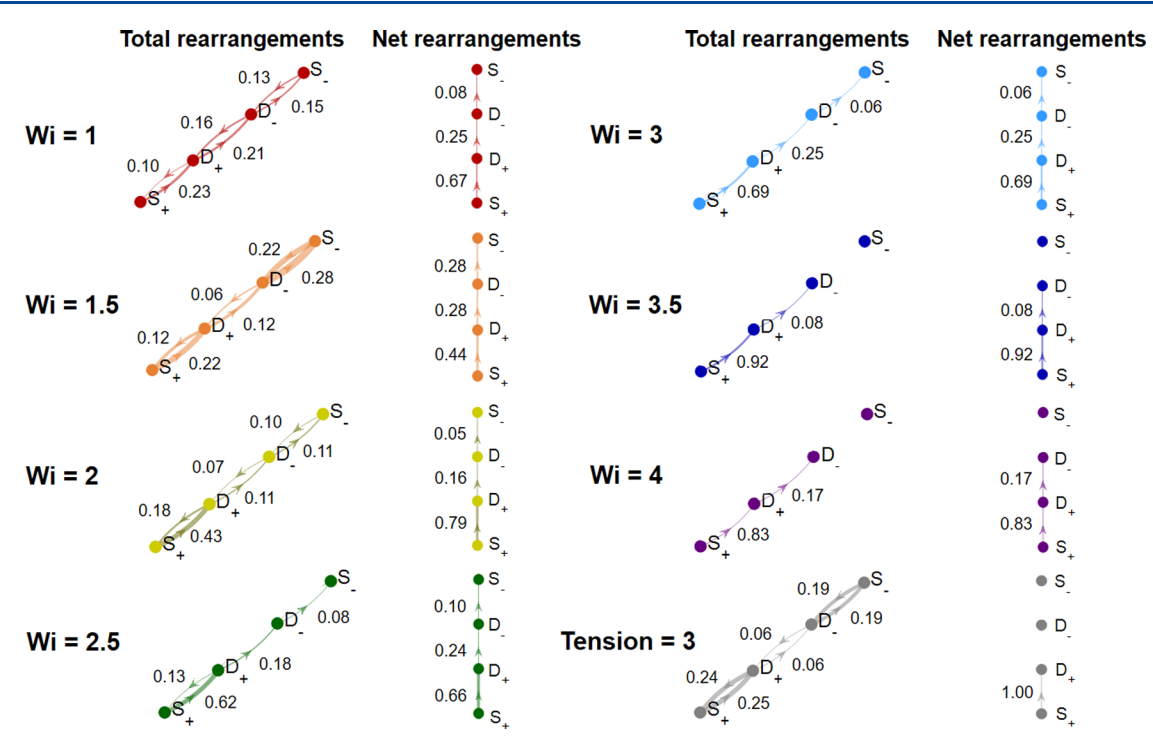


Figure 3. Total and net rearrangements of the 8_1 knot in elongational flows at different Wi. The isotension case is shown for comparison purposes. The width of each total and net rearrangement is weighted by the observed number of occurrences. The numbers indicate the fractional counts of each rearrangement type.

profile along a chain in an elongational flow is non-uniform (see the Supporting Information for tension profiles), as an initially centered knot moves off the chain, the knot swells due to the decrease in chain tension away from the center of the chain. The presence of a knot serves to reduce the effective contour length of a chain, which results in a faster polymer relaxation time and, consequently, a lower effective Wi.⁴ At a low Wi, the change in effective Wi during the untying process can induce the chain to undergo a transition from a stretched to coiled state and the knot primarily diffuses off the chain (diffusion-driven);³⁸ at a high Wi, the knot is convected off the chain beyond a critical length scale away from the center of the chain (convection-driven). Although the untying of a knot in an elongational flow is initiated by convection of the knot off the chain, due to the dynamic changes in knot size and chain extension as the knot moves off the chain, the unknotting process can be driven by diffusion or convection.¹⁷

Due to the non-uniform tension profile along a chain in elongational flow, we expect the distribution of knot conformational states at the center of the chain to be different from that at the end of the chain. Specifically, the 81 knot should take on more S states at the center of the chain where tension is at a maximum, compared to at the chain ends where tension approaches zero. Figure 2 shows the distributions of conformational states for the 81 knot at the center and end of chains in elongational flows at different Wi values, with the distributions on chains subjected to constant tension $\tilde{F}_{\rm T} = F_{\rm T} l/k_{\rm b} T = 3$ shown for comparison. This constant tension value is comparable to the average of mean chain tensions in the range of Wi investigated and is approximately the tension at the center of a chain in an elongational flow at Wi = 1.5. Across all Wi, we observe that the 8_1 knot primarily takes on either the S₊ or S₋ state at the center of the chain. This is more apparent with chains at higher Wi since peak

chain tension increases with Wi, which is consistent with our previous study that showed the S state to be favored at higher tensions.³⁰ We note that the knots studied in this work are fully equilibrated, such that the distributions of knot conformational states immediately after equilibration are independent of the initial conformational state (Figure S4).

As initially centered knots convect off the chain and move from regions of higher to lower tension, we expect the distribution of knot conformational states to generally shift from the S_+ and S_- states to the D_+ and D_- states. However, as seen from Figure 2, the observed shift in conformational states as knots move from the center to end of the chain is mainly from the S_+ state to the D_+ and D_- states for all Wi. At a certain Wi, most evidently Wi = 1.5, there is even an increase in the proportion of S_- states at the end compared to the center of the chain. In comparison, the distributions of knot conformational states on uniformly tensioned chains are similar at the center and end of the chain, and correspond to the equilibrium distribution of conformational states for the S_1 knot at applied tension $\tilde{F}_T = 3$.

To further investigate the shift in conformational states on chains in elongational flows, we consider all conformational state rearrangements that occur as initially centered knots move off the chains (Figure 3). Each conformational state of the 8₁ knot is accessible from another via rotation of the loop about the clasp of the knot, a move that brings a twist from one end of the knot to the other (see the Supporting Information for visual illustration and movie demonstration). A knot in the S₊ state can rearrange to the D₊ state, which can be further rearranged to give the D₋ state followed by the S₋ state. Rotation of the loop about the clasp in the opposite direction results in the reverse rearrangements. As seen from the net conformational state rearrangements presented in Figure 3, the 8₁ knot exhibits a primary net rearrangement pathway across

all Wi in elongational flows: $S_+ \to D_+ \to D_- \to S_-$. This is contrary to what was anticipated, that there would be net rearrangements from both the S_+ and S_- states to the D_+ and D_- states.

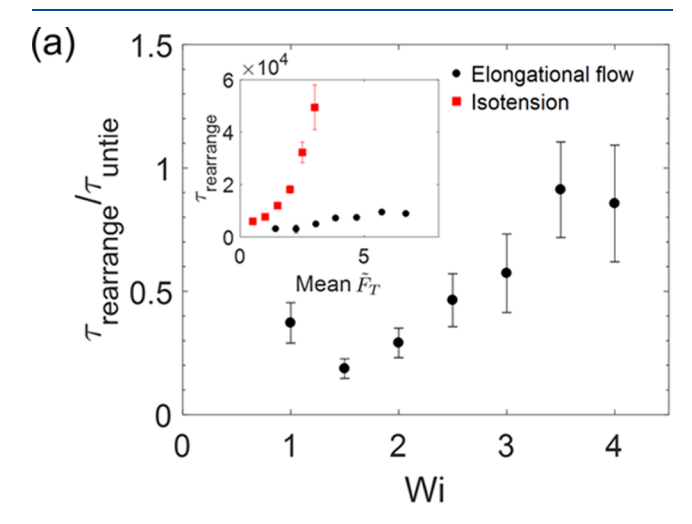
Based on Figure 3, as the 81 knots translate along the chain and move from regions of higher to lower tension, the S₊ state is a net conformational state source and the S_ state a net sink. We believe that the primary net rearrangement pathway exhibited by the 81 knot on chains in elongational flows arises from the motion of the knot during convection off the chain. A previous study by our group 16 investigated the motion of knots on chains in elongational flows at high Wi and found that knots take on a rotational mode of motion that aids translation along the chain. Given that each conformational state of the 81 knot is accessible from another through rotation of certain strands within the knot relative to others, we deduce that global rotation of the knot promotes local rotation that results in the rearrangement of conformational states. We conjecture that the observed direction of the primary net rearrangement pathway, S₊ to S₋ and not vice versa, is attributable to the conformational state rearrangement that facilitates translation of the knot along the chain. Conformational state rearrangement of the 81 knot involves moving a twist from one end of the knot to the other, which effectively results in the knot moving toward the side that the twist is moved to. For a knot in the S₊ state, this helps to move it in the direction of convection, whereas for a knot in the S_{_} state, rearrangement of conformational states is counterproductive to its translation along the chain.

It is interesting to note that the 8_1 knot exhibits the primary net rearrangement pathway for all Wi, despite the untying process being in the diffusion-driven regime at low Wi (a previous study by our group found Wi = 1.5 to be the onset of the convection-driven regime for the 8_1 knot¹⁷), suggesting that even a small contribution of convection to knot motion is sufficient to drive the knot to rearrange in a preferred manner. For knots on uniformly tensioned chains that undergo purely diffusive motion, we observe roughly balanced rearrangements between the different conformational states, such that there are almost no net rearrangements. This is consistent with the observation of similar distributions of conformational states regardless of knot location along chains subjected to constant tension

In an elongational flow, as Wi increases and the convective contribution to knot motion becomes larger, the rearrangements tend more toward the primary net rearrangement pathway. Comparing all the knot conformational state rearrangements that occur at Wi = 1 and Wi = 3, we find that knots at Wi = 1 experience all possible types of rearrangements with slight biases toward the primary net rearrangement pathway, whereas knots at Wi = 3 undergo rearrangements dictated by the primary net rearrangement pathway without any rearrangements in the reverse direction. Being in the convection-driven unknotting regime, knots at a higher Wi are expected to have faster global rotation timescales, but this does not translate into faster conformational state rearrangement timescales despite conformational state rearrangements being promoted by global rotation of the knot. The rearrangement of conformational states is an activated process and requires a thermal fluctuation to overcome the activation barrier, and thermal fluctuations are suppressed at higher chain tensions.³⁰ For Wi > 3, due to the comparable timescales for knot convection off the chain and

rearrangement of conformational states, the knots are unable to fully traverse the primary net rearrangement pathway.

3.2. Conformational State Rearrangement Time. Figure 4a shows the mean conformational state rearrangement



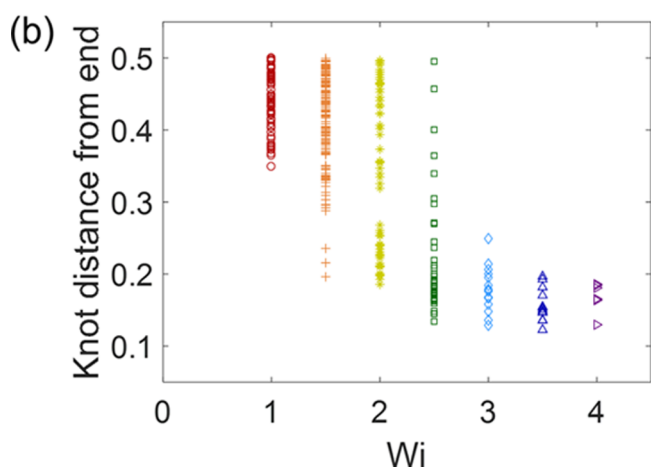


Figure 4. (a) Mean conformational state rearrangement time rescaled by mean knot untying time for the 8_1 knot on chains in elongational flows as a function of Wi. Inset: Mean conformational state rearrangement time as a function of mean chain tension for the 8_1 knot on chains in elongational flows and under constant tension. Error bars represent standard error of the mean. (b) Normalized distances between knot positions where conformational state rearrangements occur and chain ends for each Wi.

time rescaled by mean untying time for the 81 knot on chains in elongational flows as a function of Wi. The conformational state rearrangement time is the time spent in each conformational state excluding the final conformational state before the knot unties, and the knot untying time is the elapsed time between the start of the simulation and when the calculated Alexander polynomial first changes (when the knot first reaches a chain end). From Wi = 1 to Wi = 1.5, we observe a decrease in the rescaled rearrangement time, attributable to the unknotting process transitioning from the diffusion-driven to the convection-driven unknotting regime that leads to a significant increase in knot untying time (Figure S6). This is in agreement with a previous study from our group that determined Wi = 1.5 to be the onset of the convection-driven regime for the 8₁ knot.¹⁷ The ratio of mean rearrangement time to mean untying time reaches a minimum at Wi = 1.5,

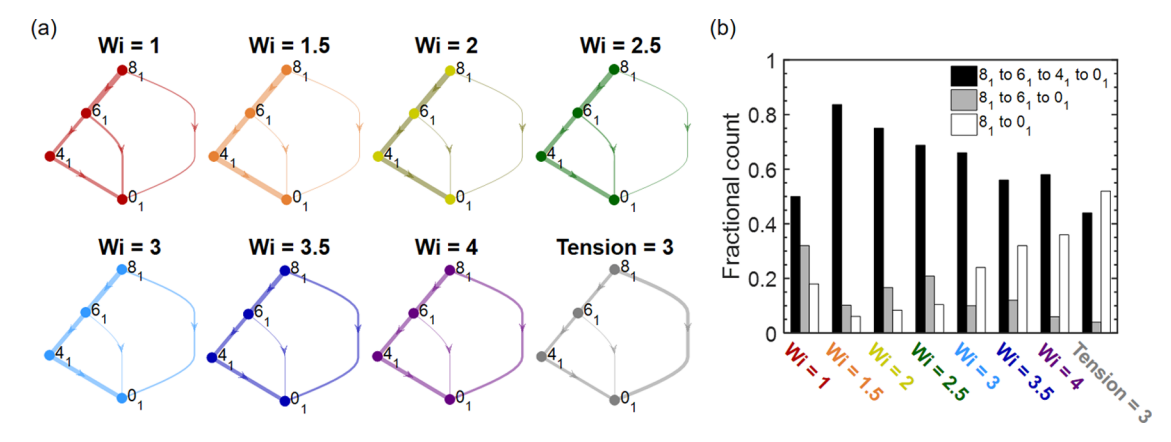


Figure 5. Distributions of untying pathways for the 8_1 knot in elongational flows at different Wi in (a) directed graph and (b) bar chart format. The width of each untying pathway in (a) is weighted by the observed number of occurrences. The isotension case is shown for comparison purposes. An ensemble of 50 chains was run for each Wi.

which indicates that the knot goes through the most number of conformational state rearrangements at this flow strength.

Beyond Wi = 1.5, there is a general increase in rearrangement time relative to knot untying time with increasing Wi. This is in accordance with expectation that knots at a higher Wi undergo conformational state rearrangements closer to the chain ends, given the decrease in rate of conformational state rearrangement with increased chain tension³⁰ and the approximately quadratic tension profile of chains in elongational flows. At high Wi, the rescaled mean rearrangement time levels off at approximately 90%. The presence of a plateau suggests that the zero tension at chain ends in elongational flows is key for allowing knots at a high Wi to undergo conformational state rearrangements. Comparing the mean rearrangement times on chains in elongational flows with mean rearrangement times on chains held at constant tension (Figure 4a, inset), we find that a knot on a chain in an elongational flow undergoes conformational state rearrangements on a much faster timescale compared to a knot held on a uniformly tensioned chain with the same mean tension. For example, a knot on a chain at Wi = 2 (mean chain tension $\overline{F}_{\rm T}$ = 3.1) goes through conformational state rearrangements at a rate of 7.3×10^{-5} (number of rearrangements per unit time), compared to a knot on a chain held at constant tension $F_T = 3$ at a rate of 8.0×10^{-6} . Indeed, the mean rearrangement time scales exponentially with chain tension for knots on uniformly tensioned chains, a trend not observed with knots on chains in elongational flows.

The faster rearrangement timescales for knots on chains in elongational flows compared to knots on uniformly tensioned chains results from the ends of chains in elongational flows having zero tension. Regardless of what the mean tension is along the chain, the knot always traverses a region of low tension as a chain end is approached. In Figure 4b, we present the normalized distances between knot positions at which conformational state rearrangements for the 81 knots occur and chain ends for each Wi. The position of the knot is taken to be the midpoint index of the knot and the distance between the knot and chain end is normalized by the chain length. At low Wi, the knots undergo conformational state rearrangements along the entirety of the chain. As Wi is increased, the positions at which rearrangements occur shift toward the ends of the chain, with the rearrangements at Wi = 3.5 and Wi = 4taking place solely near the chain ends. Despite the chains in

elongational flows of Wi = 3.5 and Wi = 4 having high mean tensions (\tilde{F}_T = 5.7 and 6.7 respectively), conformational state rearrangements can still occur due to the chain ends having zero tension.

3.3. Knot Untying Pathway. The primary net conformational state rearrangement pathway exhibited by the 8_1 knot in an elongational flow gives rise to a dominant untying pathway for the knot. As detailed in Section 3.2, the way in which the 8_1 knot unties depends on its conformational state when it reaches a chain end. Due to the 8_1 knot tending to shift from the S_+ state toward the S_- state in an elongational flow, the majority of knots are in the S_- state when a chain end is reached. In the S_- state, the 8_1 knot unties in three steps, with each step involving the removal of a twist from the knot. Assuming no further conformational state rearrangements by the partially untied knot, the 8_1 knot first partially unties into the 6_1 knot, followed by the 4_1 knot and then the 0_1 knot, or unknot (Figure 1d).

Figure 5 shows distributions of the untying pathways for the 81 knot on chains in elongational flows at different Wi. For all Wi considered, we observe the $8_1 \rightarrow 6_1 \rightarrow 4_1 \rightarrow 0_1$ untying pathway to be dominant. At Wi = 1, the dominant untying pathway constitutes approximately 50% of the observed untying pathways. The proportion of untying pathways accounted for by the dominant pathway reaches a maximum at Wi = 1.5, which marks the transition between the diffusiondriven and convection-driven regimes for the unknotting process. This is consistent with the observation that the largest proportion of knots are in the S_ state at the chain end for Wi = 1.5, as shown in Figure 2. As Wi increases, the increased mean tension along the chain leads to a decrease in number of conformational state rearrangements (Figure 4); hence, fewer knots have sufficient time to traverse the entirety of the primary net rearrangement pathway. This is reflected in the decrease in observed proportion of the $8_1 \rightarrow 6_1 \rightarrow 4_1 \rightarrow 0_1$ untying pathway and simultaneous increase in the proportion of the $8_1 \rightarrow 0_1$ pathway, which results from the knot being in the S₊ state. We note that a knot held at constant tension has a roughly equal probability of untying by the $8_1 \rightarrow 6_1 \rightarrow 4_1 \rightarrow 0_1$ and $8_1 \rightarrow 0_1$ pathways, in agreement with the notion that a knot undergoing diffusive motion has no bias in conformational states $(S_+$ versus $S_-)$. Evidently, the topological simplification of an untying knot is strongly influenced by the flow kinematics. In particular, the untying of the 8₁ knot in

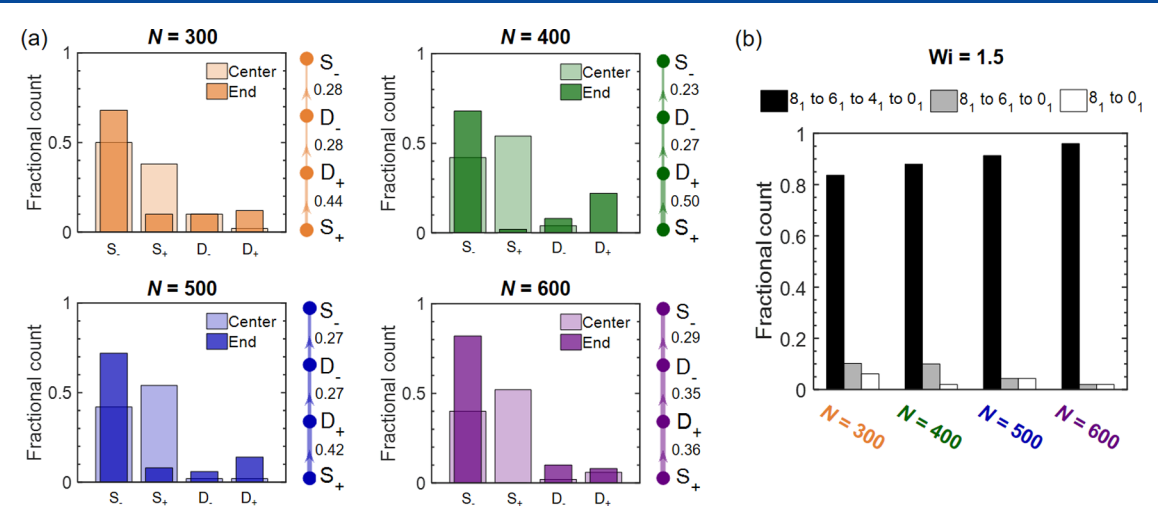


Figure 6. (a) Distributions of conformational states at the center versus end of the chain and net conformational state rearrangement pathways for the 8_1 knot in elongational flow at Wi = 1.5 for different chain lengths. The width of each net rearrangement is weighted by the observed number of occurrences. The numbers indicate the fractional counts of each net rearrangement. (b) Distributions of untying pathways for the 8_1 knot in elongational flow at Wi = 1.5 for different chain lengths. An ensemble of 50 chains was run for each chain length.

a planar elongational flow tends to occur over the most number of untying steps possible.

3.4. Changing Chain Length. The results discussed thus far have been limited to a particular chain length (N=300 beads). Next, we investigate the untying of knots on chains of varying lengths while keeping Wi constant. An increase in chain length at constant Wi leads to an increase in knot untying time. Hence, we expect that a knot on a longer chain has more time to undergo conformational state rearrangements before the knot reaches the end of the chain and unties.

Figure 6a shows the distributions of conformational states at the center and end of chains in elongational flow at Wi = 1.5 for the 8_1 knot on chains with N = 300-600 beads, along with the net conformational state rearrangement pathways. With an increase in chain length, the knots evidently go through more conformational state rearrangements, which brings about more rearrangements along the primary net rearrangement pathway. Notably, the distribution of conformational states at the center of a chain with N = 300 beads consists of 38% S₊ state and 50% S_ state, which changes to 10% and 68% for the S₊ and S_ states, respectively, at the end of the chain, while the distribution on a chain with N = 600 beads shifts from 52% and 40% to 0% and 82% for the S₊ and S₋ states, respectively, at the center versus end of the chain. More rearrangements along the primary net rearrangement pathway leads to knots generally being closer to the S_{-} state than the S_{+} state at chain ends, the result being that more knots untie via the dominant untying pathway. As seen in Figure 6b, the proportion of knots that exhibit the dominant untying pathway of $8_1 \rightarrow 6_1 \rightarrow 4_1 \rightarrow 0_1$ increases with increasing chain length, increasing from 84% for chains with N = 300 beads to 96% for chains with N = 600 beads. It can be inferred that the probability of the 81 knot untying by the dominant untying pathway in an elongational flow tends to 100% as the chain becomes infinitely long. We note that the dependence of untying pathways on chain length is likely to be different in the limit of diffusion-driven unknotting, which was considered in a previous study by our group.31

3.5. Beyond the Model Knot. To this point, we have focused on the conformational state rearrangements and consequences on the untying pathway solely for the model

8₁ knot. We proceed to consider if the observed behavior can be more broadly generalized to other knots. As was done in our previous study,³⁰ because defining and inspecting all possible conformational states for other knots would require considerable effort, we opt to gain insight instead by examining the untying pathways of different knots in elongational flow.

For this work, we choose to generalize our findings to the family of twist knots for various reasons. First, torus knots and twist knots are considered to be the simplest knot types. Considering all prime knots with up to 10 crossings, most of the torus knots are (p,2)-torus knots, which can only untie via one pathway³⁹ and are accordingly not of interest for the purposes of this study. Hence, twist knots represent the simplest family of knots with rich untying pathways for exploration. Second, twist knots are commonly found in nature, likely due to the ease with which such knots can be formed and untied. All twist knots have an unknotting number of one, meaning that the knot has to cross itself a minimum of one time to fully untie. Conversely, a twist knot can be formed by crossing itself just one time. As examples of the ubiquity of twist knots, the enzyme type II topoisomerase directs the formation of twist knots in DNA molecules⁴⁰ and knots found in proteins are primarily twist knots. 41,42

Figure 7 shows the distributions of untying pathways for three twist knots (the 7₂ knot, 9₂ knot, and 10₁ knot) on chains in elongational flow at Wi = 3, with the untying pathways on uniformly tensioned chains shown for comparison purposes (see Tables S1-S3 for data). We observe that all three twist knots exhibit dominant untying pathways when subjected to elongational flow, but not when held under constant tension, in agreement with the results discussed for the 81 knot in Section 3.3. The dominant untying pathways of the knots are analogous to the $8_1 \rightarrow 6_1 \rightarrow 4_1 \rightarrow 0_1$ untying pathway for the 81 knot, based on which we can infer that the knots undergo preferred conformational state rearrangements during convection off the chain. The twists of the knots are moved from one side of the knot to the other, in the same direction as knot translation along the chain, such that the knots tend toward the conformational state analogous to the S_ state for the 81 knot. This results in the knots primarily untying by the longest

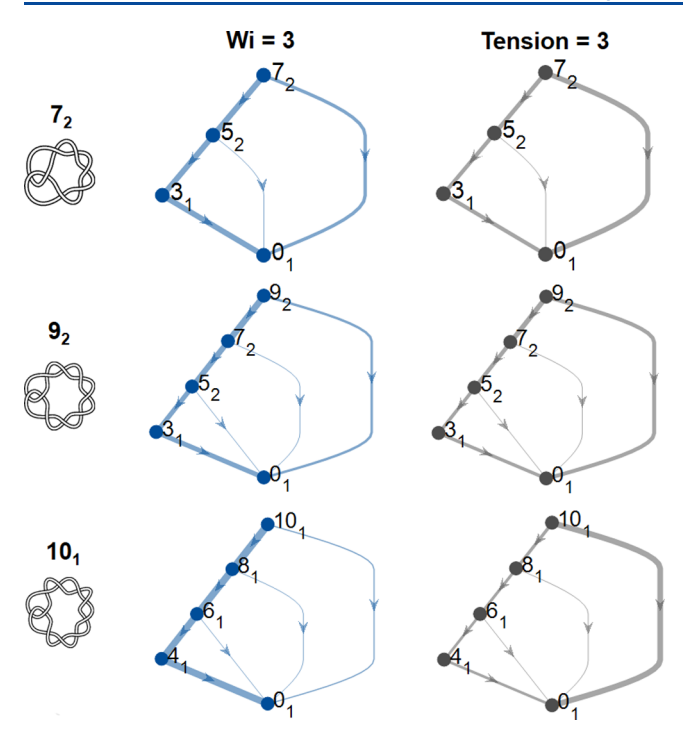


Figure 7. Distributions of untying pathways for the 7_2 knot, 9_2 knot and 10_1 knot on chains in elongational flow at Wi = 3 and under constant tension $\tilde{F}_T = 3$. The width of each untying pathway is weighted by the observed number of occurrences. An ensemble of 50 chains was run for each set of conditions.

topological pathway available, similar to what was observed with the $\mathbf{8}_1$ knot.

We highlight that, because partially untied twist knots are also twist knots, the biased rearrangement of knots in elongational flows that leads to a primary net rearrangement pathway and dominant multi-step untying pathway is a compounded effect. As an example, we consider a 81 knot that reaches a chain end in the D₊ state. The knot would partially untie into the 61 knot and be in the conformational state analogous to the S_+ state for the 8_1 knot (net conformational state source). Based on the results discussed in this section, we understand that the partially untied 61 knot would have a tendency to rearrange conformational states toward the analog for the S_ state (net conformational state sink), which would then result in the same untying pathway as a 81 knot that had reached a chain end in the S_ state. Among the 81 knots that reach a chain end in the D+ state in elongational flow at Wi = 3, we find that 88% (seven out of eight cases) until via the $8_1 \rightarrow 6_1 \rightarrow 4_1 \rightarrow 0_1$ pathway nonetheless. Therefore, even though the knot might not fully traverse the primary net rearrangement pathway before untying, it can still untie via the dominant untying pathway due to further conformational state rearrangement of the partially untied knot.

For next-generation DNA mapping and sequencing technologies, the overarching goal is to analyze large DNA molecules with lengths on the order of 100 μ m, but the inevitable presence of knots can lead to errors. The knots can be removed by subjecting the molecules to external flows, in particular planar elongational flows. The chain lengths considered in this work range from N=300 to 600 beads, equivalent to polymer chains with lengths between 3 and 6 μ m. Given the ubiquity of twist knots, coupled with the chain

lengths of interest, we can infer that many knots found in DNA molecules will only fully untie after multiple untying steps when subjected to elongational flows.

4. CONCLUSIONS

In this work, we used Brownian dynamics simulations to study the conformational states of the 81 knot on chains in planar elongational flows and the implications for the topological pathways of the untying knots. Due to the non-uniform tension profile along a chain in elongational flow, the distribution of knot conformational states is vastly different at the center versus end of the chain. By tracking all changes in conformational states as initially centered knots move off chains in elongational flow, we showed that the knots exhibit a primary net conformational state rearrangement pathway, a phenomenon not observed with knots on uniformly tensioned chains. We believe that the primary net rearrangement pathway is promoted by the rotational mode of motion experienced by knots when convected along chains in elongational flow. As Wi is increased (decreased), the convective contribution to knot motion becomes larger (smaller) and the net rearrangement pathway becomes more (less) pronounced. The rearrangement of conformational states occurs on much faster timescales for knots on chains in elongational flows compared to knots on uniformly tensioned chains, attributable to the regions of low tension near chain ends. As a result of the knots undergoing a primary net rearrangement pathway in elongational flow, a large proportion of knots take on a specific conformational state by the time a chain end is reached, and consequently, there is a dominant topological pathway by which the knots untie. We demonstrated the effect to be enhanced on longer chains, on which knots have more time to rearrange conformational states before untying. To generalize our findings, we considered the untying pathways of other twist knots in elongational flow.

The prevalence of knots across multiple length scales in our daily lives has led to interest in not only the mechanism of knotting on chains but also the process of unknotting. This study has shown that knots on chains in elongational flows can present rich untying dynamics that differ significantly from knots on uniformly tensioned chains. From an application in biotechnology perspective, flow kinematics can be used to direct the way in which a knot unties in single-molecule technologies. Looking forward, we hope that this work can inspire further studies on the unknotting of chains in flow fields.

ASSOCIATED CONTENT

Supporting Information

The Supporting Information is available free of charge at https://pubs.acs.org/doi/10.1021/acs.macromol.0c01322.

Visual illustrations of untying pathways and conformational state rearrangements for 8₁ knot, chain tension profiles, knot untying time and data for untying pathways (PDF, MP4)

Representative simulation movies of the 8_1 knot untying in planar elongational flows of varying strengths (Wi = 1, Wi = 2, Wi = 3, and Wi = 4) (MP4, MP4, MP4, MP4)

AUTHOR INFORMATION

Corresponding Author

Patrick S. Doyle — Department of Chemical Engineering, Massachusetts Institute of Technology, Cambridge, Massachusetts 02139, United States; orcid.org/0000-0003-2147-9172; Email: pdoyle@mit.edu

Authors

Beatrice W. Soh – Department of Chemical Engineering, Massachusetts Institute of Technology, Cambridge, Massachusetts 02139, United States; orcid.org/0000-0001-8399-5995

Alexander R. Klotz – Department of Physics and Astronomy, California State University, California 90840, United States

Complete contact information is available at: https://pubs.acs.org/10.1021/acs.macromol.0c01322

Notes

The authors declare no competing financial interest.

ACKNOWLEDGMENTS

We acknowledge Robert Scharein of KnotPlot for the knot diagrams. This work was supported by the National Science Foundation (NSF) grant CBET-1936696. B.W.S. is funded by the Agency for Science, Technology and Research (A*STAR), Singapore.

REFERENCES

- (1) Nureki, O.; Shirouzu, M.; Hashimoto, K.; Ishitani, R.; Terada, T.; Tamakoshi, M.; Oshima, T.; Chijimatsu, M.; Takio, K.; Vassylyev, D. G.; Shibata, T.; Inoue, Y.; Kuramitsu, S.; Yokoyama, S. An Enzyme with a Deep Trefoil Knot for the Active-Site Architecture. *Acta Crystallogr., Sect. D: Biol. Crystallogr.* **2002**, *58*, 1129–1137.
- (2) Virnau, P.; Mirny, L. A.; Kardar, M. Intricate Knots in Proteins: Function and Evolution. *PLoS Comput. Biol.* **2006**, *2*, e122.
- (3) Sumners, D. W.; Whittington, S. G. Knots in Self-Avoiding Walks. J. Phys. A: Math. Gen. 1988, 21, 1689–1694.
- (4) Soh, B. W.; Narsimhan, V.; Klotz, A. R.; Doyle, P. S. Knots Modify the Coil-Stretch Transition in Linear DNA Polymers. *Soft Matter* **2018**, *14*, 1689–1698.
- (5) Soh, B. W.; Klotz, A. R.; Robertson-Anderson, R. M.; Doyle, P. S. Long-Lived Self-Entanglements in Ring Polymers. *Phys. Rev. Lett.* **2019**, *123*, No. 048002.
- (6) Plesa, C.; Verschueren, D.; Pud, S.; van der Torre, J.; Ruitenberg, J. W.; Witteveen, M. J.; Jonsson, M. P.; Grosberg, A. Y.; Rabin, Y.; Dekker, C. Direct Observation of DNA Knots Using a Solid-State Nanopore. *Nat. Nanotechnol.* **2016**, *11*, 1093–1097.
- (7) Sharma, R. K.; Agrawal, I.; Dai, L.; Doyle, P. S.; Garaj, S. Complex DNA Knots Detected with a Nanopore Sensor. *Nat. Commun.* **2019**, *10*, 4473.
- (8) Sheng, Y. J.; Lai, P. Y.; Tsao, H. K. Topological Effects on Statics and Dynamics of Knotted Polymers. *Phys. Rev. E* **1998**, *58*, R1222.
- (9) Saitta, A. M.; Soper, P. D.; Wasserman, E.; Klein, M. L. Influence of a Knot on the Strength of a Polymer Strand. *Nature* **1999**, *399*, 46–48
- (10) Kivotides, D.; Wilkin, S. L.; Theofanous, T. G. Entangled Chain Dynamics of Polymer Knots in Extensional Flow. *Phys. Rev. E* **2009**, 80, No. 041808.
- (11) Matthews, R.; Louis, A. A.; Yeomans, J. M. Knot-Controlled Ejection of a Polymer from a Virus Capsid. *Phys. Rev. Lett.* **2009**, *102*, No. 088101.
- (12) Caraglio, M.; Micheletti, C.; Orlandini, E. Stretching Response of Knotted and Unknotted Polymer Chains. *Phys. Rev. Lett.* **2015**, 115, 188301.
- (13) Tubiana, L.; Rosa, A.; Fragiacomo, F.; Micheletti, C. Spontaneous Knotting and Unknotting of Flexible Linear Polymers:

- Equilibrium and Kinetic Aspects. Macromolecules 2013, 46, 3669-3678
- (14) Micheletti, C.; Orlandini, E. Knotting and Unknotting Dynamics of DNA Strands in Nanochannels. *ACS Macro Lett.* **2014**, *3*, 876.
- (15) Bao, X. R.; Lee, H. J.; Quake, S. R. Behavior of Complex Knots in Single DNA Molecules. *Phys. Rev. Lett.* **2003**, *91*, 265506.
- (16) Renner, C. B.; Doyle, P. S. Untying Knotted DNA with Elongational Flows. ACS Macro Lett. 2014, 3, 963-967.
- (17) Soh, B. W.; Klotz, A. R.; Doyle, P. S. Untying of Complex Knots on Stretched Polymers in Elongational Fields. *Macromolecules* **2018**, *51*, 9562–9571.
- (18) Klotz, A. R.; Soh, B. W.; Doyle, P. S. Motion of Knots in DNA Stretched by Elongational Fields. *Phys. Rev. Lett.* **2018**, *120*, 188003.
- (19) Lam, E. T.; Hastie, A.; Lin, C.; Ehrlich, D.; Das, S. K.; Austin, M. D.; Deshpande, P.; Cao, H.; Nagarajan, N.; Xiao, M.; Kwok, P.-Y. Genome Mapping on Nanochannel Arrays for Structural Variation Analysis and Sequence Assembly. *Nat. Biotechnol.* **2012**, *30*, 771–776.
- (20) Reisner, W.; Pedersen, J. N.; Austin, R. H. DNA Confinement in Nanochannels: Physics and Biological Applications. *Rep. Prog. Phys.* **2012**, *75*, 106601.
- (21) Möbius, W.; Frey, E.; Gerland, U. Spontaneous Unknotting of a Polymer Confined in a Nanochannel. *Nano Lett.* **2008**, *8*, 4518–4522.
- (22) Taylor, W. R. A Deeply Knotted Protein Structure and How It Might Fold. *Nature* **2000**, *406*, 916–919.
- (23) Yeates, T. O.; Norcross, T. S.; King, N. P. Knotted and Topologically Complex Proteins as Models for Studying Folding and Stability. *Curr. Opin. Chem. Biol.* **2007**, *11*, 595–603.
- (24) Sułkowska, J. I.; Sułkowski, P.; Szymczak, P.; Cieplak, M. Untying Knots in Proteins. J. Am. Chem. Soc. 2010, 132, 13954–13956.
- (25) Ziegler, F.; Lim, N. C. H.; Mandal, S. S.; Pelz, B.; Ng, W.-P.; Schlierf, M.; Jackson, S. E.; Rief, M. Knotting and Unknotting of a Protein in Single Molecule Experiments. *Proc. Natl. Acad. Sci. U. S. A.* **2016**, *113*, 7533–7538.
- (26) Stolz, R.; Yoshida, M.; Brasher, R.; Flanner, M.; Ishihara, K.; Sherratt, D. J.; Shimokawa, K.; Vazquez, M. Pathways of DNA Unlinking: A Story of Stepwise Simplification. *Sci. Rep.* **2017**, *7*, 12420.
- (27) Ziraldo, R.; Hanke, A.; Levene, S. D. Kinetic Pathways of Topology Simplification by Type-II Topoisomerases in Knotted Supercoiled DNA. *Nucleic Acids Res.* **2019**, *47*, 69–84.
- (28) Scheeler, M. W.; Kleckner, D.; Proment, D.; Kindlmann, G. L.; Irvine, W. T. M. Helicity Conservation by Flow Across Scales in Reconnecting Vortex Links and Knots. *Proc. Natl. Acad. Sci. U. S. A.* **2014**, *111*, 15350–15355.
- (29) Kleckner, D.; Kauffman, L. H.; Irvine, W. T. M. How Superfluid Vortex Knots Untie. *Nat. Phys.* **2016**, *12*, 650–655.
- (30) Soh, B. W.; Klotz, A. R.; Dai, L.; Doyle, P. S. Conformational State Hopping of Knots in Tensioned Polymer Chains. *ACS Macro Lett.* **2019**, *8*, 905–911.
- (31) Vologodskii, A. Brownian Dynamics Simulation of Knot Diffusion along a Stretched DNA Molecule. *Biophys. J.* **2006**, *90*, 1594–1597.
- (32) Huang, J.; Schlick, T.; Vologodskii, A. Dynamics of Site Juxtaposition in Supercoiled DNA. *Proc. Natl. Acad. Sci. U. S. A.* **2001**, *98*, 968–973.
- (33) Liu, T. W. Flexible Polymer Chain Dynamics and Rheological Properties in Steady Flows. J. Chem. Phys. 1989, 90, 5826–5842.
- (34) Somasi, M.; Khomami, B.; Woo, N. J.; Hur, J. S.; Shaqfeh, E. S. G. Brownian Dynamics Simulations of Bead-Rod and Bead-Spring Chains: Numerical Algorithms and Coarse-Graining Issues. *J. Non-Newtonian Fluid Mech.* **2002**, *108*, 227–255.
- (35) Tubiana, L.; Orlandini, E.; Micheletti, C. Probing the Entanglement and Locating Knots in Ring Polymers: A Comparative Study of Different Arc Closure Schemes. *Prog. Theor. Phys. Suppl.* **2011**, *191*, 192–204.

- (36) Vologodskii, A. V.; Lukashin, A. V.; Frank-Kamenetskii, M. D.; Anshelevich, V. V. The Knot Problem in Statistical Mechanics of Polymer Chains. *J. Exp. Theor. Phys.* **1974**, *66*, 2153–2163.
- (37) Fielden, S. D. P.; Leigh, D. A.; Woltering, S. L. Molecular Knots. *Angew. Chem., Int. Ed.* **2017**, *56*, 11166–11194.
- (38) Narsimhan, V.; Klotz, A. R.; Doyle, P. S. Steady-State and Transient Behavior of Knotted Chains in Extensional Fields. *ACS Macro Lett.* **2017**, *6*, 1285–1289.
- (39) Caraglio, M.; Baldovin, F.; Marcone, B.; Orlandini, E.; Stella, A. L. Topological Disentanglement Dynamics of Torus Knots on Open Linear Polymers. *ACS Macro Lett.* **2019**, *8*, 576–581.
- (40) Wasserman, S. A.; Cozzarelli, N. R. Supercoiled DNA-Directed Knotting by T4 Topoisomerase. *J. Biol. Chem.* **1991**, 266, 20567–20573.
- (41) Taylor, W. R. Protein Knots and Fold Complexity: Some New Twists. Comput. Biol. Chem. 2007, 31, 151–162.
- (42) Flapan, E.; He, A.; Wong, H. Topological Descriptions of Protein Folding. *Proc. Natl. Acad. Sci. U. S. A.* **2019**, *116*, 9360–9369.
- (43) Reifenberger, J. G.; Dorfman, K. D.; Cao, H. Topological Events in Single Molecules of E. Coli DNA Confined in Nanochannels. *Analyst* **2015**, *140*, 4887–4894.